

Article

A Sustainable Synthetic Approach to the Indaceno[1,2-b:5,6-b']dithiophene (IDT) Core through Cascade Cyclization–Deprotection Reactions

Giacomo Forti ¹, Andrea Nitti ^{1,2} , Gabriele Bianchi ³, Riccardo Po ³ and Dario Pasini ^{1,2,*} 

¹ Department of Chemistry, University of Pavia, Via Taramelli 12, 27100 Pavia, Italy; giacomo.forti01@universitadipavia.it (G.F.); andrea.nitti@unipv.it (A.N.)

² INSTM Research Unit, University of Pavia, Via Taramelli 12, 27100 Pavia, Italy

³ New Energies, Renewable Energies and Materials Science Research Center, Eni SpA, Via Giacomo Fauser 4, 28100 Novara, Italy; gabriele.bianchi1@eni.com (G.B.); riccardo.po@eni.com (R.P.)

* Correspondence: dario.pasini@unipv.it

Abstract: Bulk heterojunction organic solar cells (BHJs) are competitive within the emerging photovoltaic technologies for solar energy conversion because of their unique advantages. Their development has been boosted recently by the introduction of nonfullerene electron acceptors (NFAs), to be used in combination with a polymeric electron donor in the active layer composition. Many of the recent advances in NFAs are attributable to the class of fused-ring electron acceptors (FREAs), which is now predominant, with one of the most notable examples being formed with a fused five-member-ring indaceno[1,2-b:5,6-b']dithiophene (IDT) core. Here, we propose a novel and more sustainable synthesis for the IDT core. Our approach bypasses tin derivatives needed in the Stille condensation, whose byproducts are toxic and difficult to dispose of, and it makes use of cascade reactions, effectively reducing the number of synthetic steps.

Keywords: organic photovoltaics; nonfullerene acceptors; cascade reactions; sustainable chemistry



Citation: Forti, G.; Nitti, A.; Bianchi, G.; Po, R.; Pasini, D. A Sustainable Synthetic Approach to the Indaceno[1,2-b:5,6-b']dithiophene (IDT) Core through Cascade Cyclization–Deprotection Reactions. *Chemistry* **2022**, *4*, 206–215. <https://doi.org/10.3390/chemistry4010018>

Academic Editor: Bartolo Gabriele

Received: 14 February 2022

Accepted: 18 March 2022

Published: 21 March 2022

Publisher's Note: MDPI stays neutral with regard to jurisdictional claims in published maps and institutional affiliations.



Copyright: © 2022 by the authors. Licensee MDPI, Basel, Switzerland. This article is an open access article distributed under the terms and conditions of the Creative Commons Attribution (CC BY) license (<https://creativecommons.org/licenses/by/4.0/>).

1. Introduction

Among the organic photovoltaic device family, bulk heterojunction solar cells (BHJs) have developed amongst the most promising and efficient emerging technologies for solar energy conversion, because of their flexibility, stretchability, and the possibility to be integrated into many diverse materials [1–3]. BHJs usually possess a “sandwich” structure, in which the photoactive layer, made by a blended mixture of an electron donor material, usually a conjugated organic polymer, as the p-type semiconductor, and an electron acceptor small molecule (SMA) as the n-type semiconductor, is encapsulated between two interlayers—an electron-transporting layer (ETL) and a hole-transporting layer (HTL) [4,5]. Recently, the focus on the development of organic solar cells has shifted to nonfullerene electron acceptors (NFAs) as the SMA in combination with the polymeric electron donor in BHJs. In fact, the photoconversion efficiencies (PCEs) of such cells have increased dramatically since 2015, now reaching a high value of over 20% [6]. Ideal NFAs exhibit (a) strong absorption coefficients in regions of the visible and NIR spectrum that are complementary to those in which the available electron-donor polymers absorb, (b) suitably matched energy levels for achieving photoinduced charge separation with donors, (c) the ability to form appropriate morphologies for charge separation and suitable percolation pathways for charge transport, and (d) good molecular and morphological thermal and photostability. A wide variety of material classes have been examined as NFAs [7–15]. Many of the recent advances in NFA-containing organic solar cells are attributable to the class of fused-ring electron acceptors (FREAs) [16–29], which is now predominant. FREAs are well-defined organic compounds characterized by a push–pull architecture in which

π -extended donating cores having four or more aromatic fused rings are flanked by two electron-withdrawing units (A–D–A or A–D–A–D–A molecular structures, where A and D are electron-withdrawing or electron-donating structures, respectively).

Amongst FREAs, the indacenodithiophene capped with 3-oxo-2,3-dihydro-1*H*-indene-2,1-diylidene)dimalononitrile (IDIC) family of NFAs stood out in the last five years in terms of performances. The prototypical IDIC structure and its precursors are shown in Figure 1. It is composed of an electron-donating, fused five-member-ring indaceno[1,2-*b*:5,6-*b'*]dithiophene (IDT), terminated by two electron-withdrawing units. Several IDIC NFAs have been synthesized by modification of the central electron-rich core, side chains, and end-cap groups. Despite that, the synthesis of the IDT core and its functionalization remain challenging in terms of sustainable chemistry.

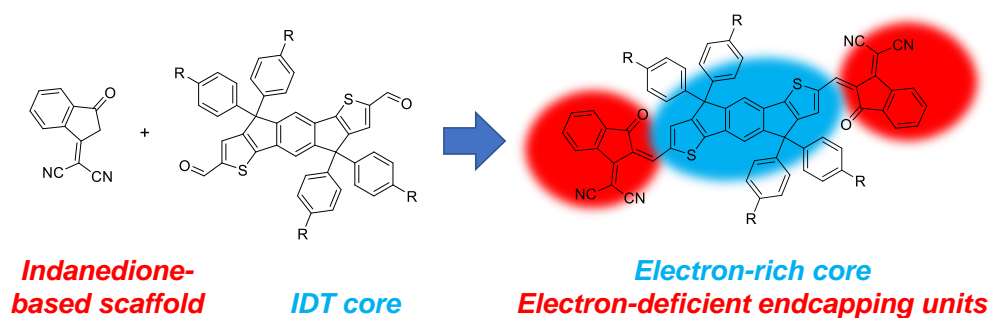


Figure 1. Structure of the prototypical IDIC NFA.

We have recently reported innovative methodologies for the synthesis of fused-ring π -extended heterocycles through cascade reactions and sustainable approaches [30–36]. Here, we propose a novel synthesis for the IDT core, which starts from relatively cheap starting materials and allow us to assemble a fully functionalized IDT core with a reduction in synthetic steps, compared with the synthetic routes reported in the literature. Our approach is innovative and more sustainable, especially considering two main aspects: (a) it avoids the use of tin derivatives, whose byproducts are well known to be toxic, and (b) it makes use of cascade reactions to reduce the number of synthetic steps.

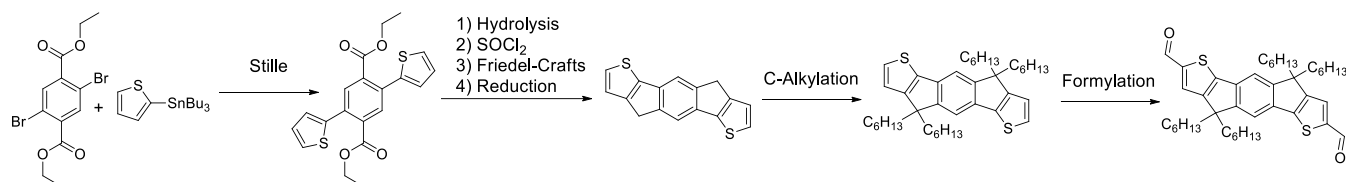
2. Results and Discussion

The two traditional main routes for the synthesis of the indaceno[1,2-*b*:5,6-*b'*]dithiophene (IDT) scaffold present in the literature are described in Scheme 1, top. They both require several steps, harsh conditions, and toxic reagents, so that large-scale production, despite the high performance shown in devices, remains unforeseeable. They both involve an initial Stille coupling of a monostannylated thiophene residue. The route developed by Luscombe et al. [37] for the IDT scaffold is followed by a series of steps involving ester hydrolysis, an intramolecular acid-catalyzed cyclization, and a reduction, followed by the alkylation of the newly formed CH₂ positions with long alkyl chains for imparting overall solubility and processability to the final product. The final step, the formylation of the terminal thiophene residues in the α -position, has been reported by other groups [38] with the use of POCl₃/DMF and affords the final IDT core, ready to be fully functionalized via a Knoevenagel reaction with the electron-deficient indanedione-based derivatized scaffold. The route developed by Jen et al. [39] for the IDT scaffold, instead, proceeds through the formation of tertiary alcohol, obtained by the double addition of an organometallic Grignard nucleophile to the ester, which is followed by acid-catalyzed cyclization. Such cascade sequence allows aryl substituents to be directly placed onto the IDT scaffold, able to impart solubility and avoid intermolecular aggregation. Additionally, in this case, the final step involves the formylation of the terminal thiophene residues in the α -position and has been reported by other groups [40] with the use of *n*-BuLi and DMF to afford the IDT core ready for the final Knoevenagel step. Other approaches have appeared in the literature [41–43], which include the use of boron chemistry. The approach presented here

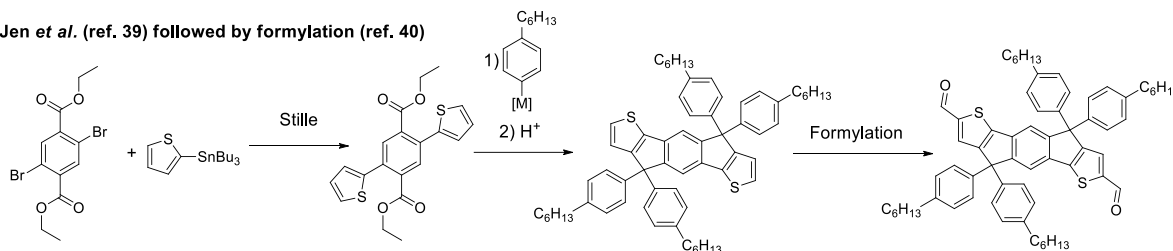
inverts the introduction of the formyl groups. Instead of introducing them in a final step, they feature in the thiophene starting materials in the protected form, and the advantage is given by the fact that the thiophene synthon we used is commercially available.

Previous syntheses

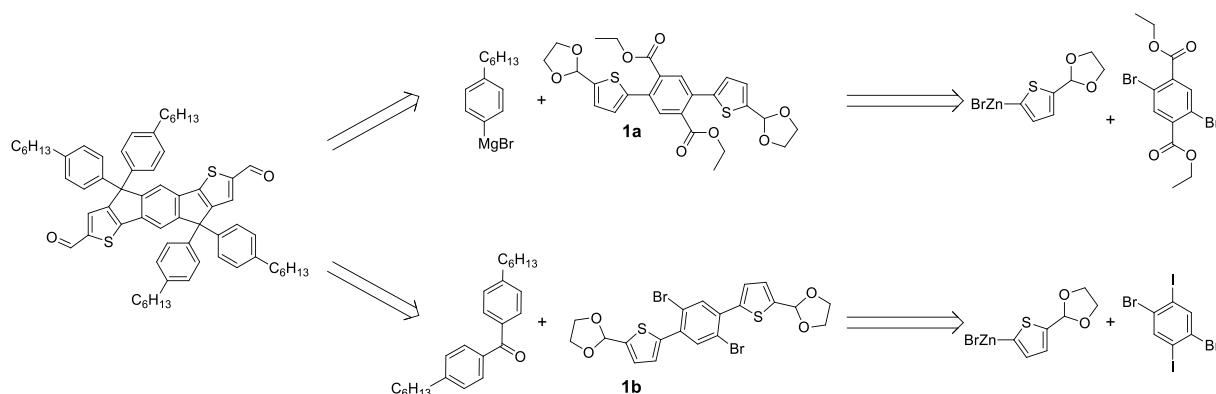
Luscombe *et al.* (ref. 37) followed by formylation (ref. 38)



Jen *et al.* (ref. 39) followed by formylation (ref. 40)



Our approach (retrosynthesis)

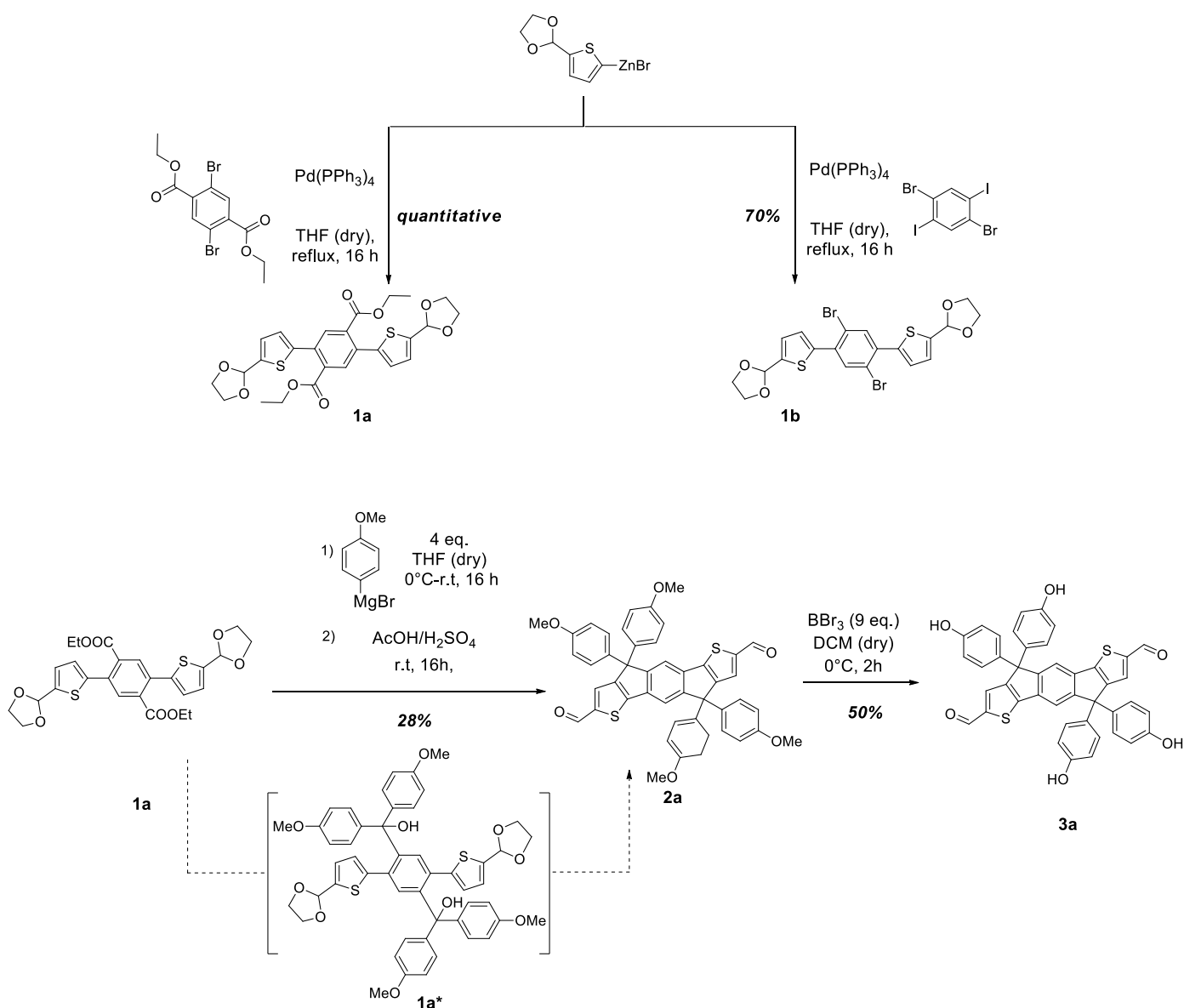


Scheme 1. (Top): previous synthetic approaches to the IDT core. (Bottom): retrosynthetic approach, this study [37–40].

We aimed to achieve a more sustainable and expeditious approach to the IDT core, to further elaborate on the cascade reaction protocol elaborated by Jen *et al.*, and to focus on alternatives to the Stille reaction used in the first step. In fact, we discovered that 5-(1,3-dioxolan-2-yl)-2-thienylzinc bromide is a commercially available starting material, sold at a reasonable price (ca. 35 EUR/g from commercial sources). Such zinc derivative as starting material, bearing an acetal into its molecular structure, allowed us to bypass the conventional route based on Stille reaction in favor of an eco-friendlier Negishi reaction for the synthesis of both diester and dibromo aryl derivatives **1a** and **1b** (Scheme 1, bottom). Compound **1a** is prone to react with an aryl Grignard reagent, and the resulting tertiary alcohol could undergo acid-catalyzed intramolecular cyclization to yield the target IDT core. Moreover, the presence of the acetal ensures, in the final acid-catalyzed cyclization step, its deprotection, to restore the aldehyde functionality without the need for a further, subsequent synthetic step, the final formylation. Compound **1b** could react, in an inverted fashion, by generating the nucleophile on the linear scaffold. Attack on a secondary ketone would generate the tertiary alcohol functionality, prone to undergo the acid-catalyzed intramolecular cyclization and deprotection mentioned above.

In the case of derivative **1a**, the Negishi protocol afforded the title compound in essentially quantitative yield, after purification of the reaction mixture by column chro-

matography. In the case of **1b**, the reaction was selective toward the functionalization of the iodide aryl substituents, with an overall yield of 70% after purification by column chromatography (Scheme 2, top). Column chromatography had to be carried out on deactivated silica to avoid deprotection of the acetal moieties directly into the column during the separation. The corresponding acetal **1a** was tested in the next step, the nucleophilic attack by the Grignard reagent, followed by a cascade intramolecular cyclization–deprotection step to yield the corresponding IDIC core **2a** (Scheme 2, bottom).



Scheme 2. (Top) Negishi coupling for derivatives **1a** and **1b**; (Bottom) one-pot cyclization–deprotection step in the synthesis of **2a** (through intermediate **1a***) and the deprotection to afford **3a**.

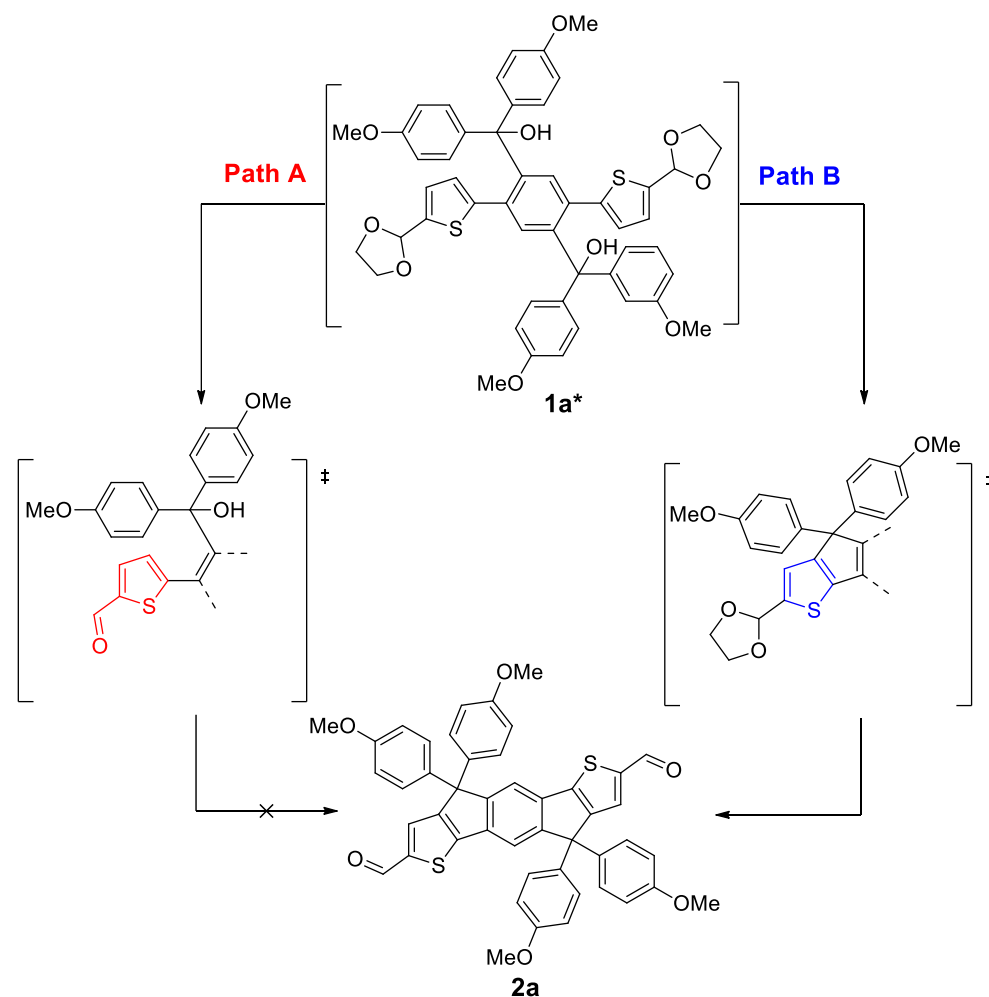
The cyclization–deprotection step has been extensively studied to find the most suitable conditions, as reported in Table 1. Noteworthy, in the classical conditions reported in the literature (entries 1 and 2), the reaction proceeded with a low yield; lowering the temperature (entry 3) allowed us to obtain derivative **2a** in a somewhat improved yet modest yield. We investigated the possibility to promote this reaction using different sources of acids: We tried SiO_2 and amberlyst as proton sources (entries 4 and 5), but after 16 h, we did not observe the formation of derivative **2a**. In the case of $\text{BF}_3 \cdot \text{OEt}_2$, after 2 h, we observed only degradation products.

Table 1. Cyclization conditions for the synthesis of **2a**.

Entry	H ⁺ Source	Conditions	Yield ¹
1	HCl/AcOH	Reflux, 3 h	7%
2	H ₂ SO ₄ /AcOH	Reflux, 3 h	7%
3	H ₂ SO ₄ /AcOH	r.t., 16 h	28%
4	SiO ₂ /H ₂ O	r.t., 16 h	-
5	Amberlyst	r.t., 16 h	-
6	BF ₃ ·Et ₂ O	0 °C to r.t., 2 h	-

¹ Isolated yield after column chromatography.

We ascribe the low yields to the consequence of competitive reaction pathways: deprotection and cyclization (Scheme 3). We speculate that, if the first reaction starting from intermediate **1a*** that occurs is deprotection (Path A), the unprotected aldehyde reduces the electron density over the thiophene ring and does not allow the intramolecular cyclization, while when the first reaction is the cyclization (Path B), the cascade reaction is ensured.



Scheme 3. Possible pathways for cyclization–deprotection step for the synthesis of compound **2a** from intermediate **1a*** through different pathways and intermediates marked with ‡.

Since the deprotection of the acetal functionality requires the stoichiometric addition of water, we performed the reaction in our best conditions (entry 3 in Table 1) in the presence of molecular sieves, with the aim of activating the acetal deprotection in the aqueous workup procedures, only after the successful cyclization had occurred. Unfortunately, yields were not improved in this case either.

In the light of the overall improved sustainability of the OPV devices, solubility and processability of the components in green solvents such as alcohols are desirable. In our approach to developing an alcoholic soluble IDT core, we deprotected molecule **2a** to restore the phenolic moiety; the demethylation reaction was carried out in presence of BBr₃ to provide the corresponding molecule **3a** (Scheme 2) in good yields. The free phenol functionalities could be functional as a solubilizing anchor for the overall core, because of their enhanced polarity and the possibility of the formation of organic salts of tunable solubility in different solvents, by using suitable cationic counterparts.

For acetal **1b**, as detailed in Scheme 1, bottom, we sought to generate the corresponding lithium derivative, followed by a reaction with several diaryl ketones. However, despite several attempts, we were never able to isolate the correct cyclized IDT core. As reported for the derivative **2a**, competition between deprotection and cyclization could be the reason for such failure, with the former pathway which, when occurring before, switches off the reactivity of the electron-rich thiophene moiety for the latter cyclization. In the case of acetal **1b**, since the correct product could not be obtained, pathway A seems to be the only one operating.

We then considered established sustainability indices such as the E factor (kg of organic waste/kg of product) [44]. E factor values for organic semiconductors are often in the excess of 10⁴, in some cases largely surpassing those for organic small molecules, which are active components of pharmaceutical formulations. Although the yield of the final step was far from optimal, E factor calculations (see Supplementary Materials) for our synthesis of molecule **2a** gave a value of 201.8. The value calculated on the conventional synthesis reported in the literature, considering the shortest route elaborated by Jen et al. (Scheme 1) on a slightly different IDT core (bearing 4-hexylphenyl aromatic spiro residues), and the formylation carried out on another slightly different IDT core (bearing 4-hexylspiro residues) [40], gave a value of 562.5. We did not include a chromatography solvent in our calculations because it can be recovered by vacuum distillation using a Rotovapor, as reported recently in the literature [45]. Our approach, therefore, allows a reduction by a factor of two of the E factor, and the synthesis is carried out in only three steps, avoiding the further formylation step required in the published approach.

3. Experimental Section

3.1. General Experimental

All commercially available reagents and solvents were purchased from Sigma-Aldrich, Fluorochem, Alfa Aesar. Flash chromatography was carried out using Merck silica gel 60 (pore size 60 Å, 270–400 Mesh). ¹H and ¹³C NMR spectra were recorded from solutions in deuterated solvents on 300 Bruker or 400 Jeol spectrometers with the residual solvent as the internal standard. Mass spectra of pure compounds were recorded using an Electron Spray Ionization Agilent Technologies mass spectrometer, a Direct Exposure Probe mass spectrometer, or a GC–MS ThermoScientific spectrometer.

3.2. Synthesis of New Compounds

2,5-bis(5-(1,3-dioxolan-2-yl)thiophen-2-yl)terephthalate (1a). In a flame dried dry Schlenk tube, under Argon, diethyl 2,5-dibromoterephthalate (1 g, 2.63 mmol), (5-(1,3-dioxolan-2-yl)thiophen-2-yl)zinc bromide (11.5 mL, 5.8 mmol), and Pd(PPh₃)₄ (122 mg, 0.105 mmol) were added in previously degassed dry THF (20 mL, 0.15 M). The resulting black solution was refluxed under stirring. After 16 h, the reaction was stopped, and the resulting solution was extracted three times with DCM/NaHCO₃ solution. The combined organic phases were dried (Na₂SO₄); then, the solvent was removed under reduced pressure to yield a dark solid, which was purified by flash chromatography (basic SiO₂, 7:3 v/v hexanes/EtOAc) to give a yellow solid in quantitative yield. ¹H NMR (300 MHz, CDCl₃): δ = 7.84 (s, 2H), 7.13–7.11 (d, 2H, J = 3.6 Hz), 6.98–6.96 (d, 2H, J = 3.5 Hz), 6.31 (s, 2H), 4.25–3.97 (m, 12H), 1.21–1.14 (t, 6H, J = 14 Hz). ¹³C NMR (101 MHz, CDCl₃): δ = 167.31, 142.91, 141.23, 133.81,

133.26, 131.82, 126.33, 126.22, 107.5, 65.15, 61.17, 13.68. ESI-MS: 553 [M + Na]⁺ (100). HRMS calculated for C₂₆H₂₆O₈S₂: 530.1069; found: 530.1078.

2,2'-(2,5-dibromo-1,4-phenylene)bis(thiophene-5,2-diyl)bis(1,3-dioxolane) (**1b**). In a flame dried dry Schlenk tube, under Argon, 1,4-dibromo-2,5-diiodobenzene (100 mg, 0.20 mmol), 5-(1,3-dioxolan-2-yl)thiophen-2-ylzinc bromide (0.9 mL, 0.45 mmol), and Pd(PPh₃)₄ (12 mg, 0.010 mmol) were added in previously degassed dry THF (2 mL, 0.1 M). The resulting black solution was stirred at 60 °C. After 1 day, the reaction was stopped, and the resulting reaction mixture was extracted with DCM/NaHCO₃ solution. The combined organic phases were dried (Na₂SO₄); then, the solvent was removed under reduced pressure to yield a black solid. The desired compound was purified by flash chromatography (basic SiO₂, 9:1 to 8:2 hexanes/EtOAc) to give a light-yellow solid (110 mg, 73%). ¹H NMR (400 MHz, CDCl₃): δ = 7.77 (s, 1H), 7.25–7.24 (d, 1H, J = 4Hz), 7.17–7.16 (d, 1H, J = 4Hz), 6.13 (s, 1H), 4.21–4.00 (m, 4H). ¹³C NMR (101 MHz, CDCl₃): δ = 143.33, 140.54, 136.01, 135.74, 128.11, 126.25, 121.16, 100.21, 65.35, 65.28. ESI-MS: 1111 [2M + Na]⁺ (100). HRMS calculated for C₂₀H₁₆Br₂O₄S₂: 541.8857; found: 541.8853.

4,4,9,9-tetrakis(4-methoxyphenyl)-4,9-dihydro-s-indaceno[1,2-b:5,6-b']dithiophene-2,7-dicarbaldehyde (**2a**). In a flame dried dry Schlenk tube, under Argon, a light-yellow solution of **1a** (246 mg, 0.46 mmol) in dry THF (3 mL, 0.15 M), the resulting solution was cooled to 0 °C; then 4-methoxyphenylmagnesium bromide (4.10 mL, 2.05 mmol) was added dropwise under stirring. The solution immediately changed its color from light yellow to red. The resulting red solution was allowed to reach r.t., under stirring. After 16 h, the reaction was stopped, and the resulting red solution was quenched with a NaHCO₃ solution and then extracted with DCM/H₂O to yield an orange solid. The resulting orange solid was dissolved at r.t. in AcOH and a catalytic amount of conc. H₂SO₄ was added, and the resulting solution immediately changed its color from orange to violet. After 16 h under stirring at r.t., the resulting violet solution was quenched with an aqueous solution of NaHCO₃ and extracted three times with DCM/H₂O. The combined organic phases were dried (Na₂SO₄), and the solvent was removed under reduced pressure to yield an orange solid. The resulting orange solid was purified by flash chromatography (7:3 v/v hexanes/EtOAc) to give compound **2a** as a yellow solid (95 mg, 28% yield). ¹H NMR (300 MHz, CDCl₃): δ = 9.87 (s, 2H), 7.63 (s, 2H), 7.58 (s, 2H), 7.18–7.14 (d, 8H, J = 8.8 Hz), 6.84–6.80 (d, 8H, J = 8.8 Hz), 3.78 (s, 12H) ppm. ¹³C NMR (75 MHz, CDCl₃) δ = 182.69, 158.77, 157.14, 155.38, 149.98, 146.44, 135.70, 135.23, 131.57, 128.71, 118.83, 113.92, 62.14, 55.17. ESI-MS: 747.33 [M + 1]⁺ (80). HRMS calculated for C₄₆H₃₆O₆S₂: 748.1953; found: 748.1955.

Synthesis of *4,4,9,9-tetrakis(4-hydroxyphenyl)-4,9-dihydro-s-indaceno[1,2-b:5,6-b']dithiophene-2,7-dicarbaldehyde* (**3a**). In a flame-dried, dry Schlenk tube, under Argon, a solution of **2a** (95 mg, 0.127 mmol) in dry DCM (1.2 mL, 0.1 M) was cooled to 0 °C; then, BBr₃ (0.980 mmol, 170 μL) was added dropwise under stirring. The solution immediately changed its color from light yellow to dark red. The resulting dark red solution was allowed to reach r.t. under stirring. After 2 h, the reaction was stopped, and the resulting dark blue solution was extracted three times with EtOAc/H₂O. The combined organic phases were dried (Na₂SO₄), and the solvent was removed under reduced pressure to yield a dark red solid. The resulting dark red solid was purified by precipitation in hexanes from THF to give **3a** as a red solid compound (44 mg, 50%). ¹H NMR (300 MHz, acetone-*d*₆): δ = 9.91 (s, 2H), 8.35 (s, 4H), 7.96 (s, 2H), 7.90 (s, 2H), 7.15–7.11 (d, 8H, J = 8.5 Hz), 6.77–6.73 (d, 8H, J = 8.6 Hz). ¹³C NMR (75 MHz, acetone-*d*₆): δ = 184.41, 157.91, 148.18, 135.78, 133.48, 130.17, 119.79, 118.69, 116.55, 55.32. HRMS calculated for C₄₂H₂₈O₆S₂: 692.1171; found: 692.1165.

4. Conclusions

We successfully developed a novel synthesis for the IDT core, which can be carried out from relatively cheap starting materials and allow us to assemble a fully functionalized indaceno[1,2-b:5,6-b']dithiophene scaffold in only three synthetic steps. Our approach is more sustainable than current approaches reported in the literature, as testified by the reduction in a commonly used green metric parameter, the E factor, by a factor of two. Two

other aspects must be stressed as evidence pointing to the decisive improvement of our procedure over existing ones: (a) our synthesis avoids the use of Stille condensation and related tin derivatives, whose byproducts are toxic and difficult to dispose of, and (b) it makes use of cascade reactions to reduce the number of synthetic steps. Further studies will focus on the possible improvement of the key cyclization–deprotection strategy, and on the possibility to use the phenolic scaffold **3a** to produce novel NFAs, which could be soluble and processable in green polar solvents such as alcohols.

Supplementary Materials: The following supporting information can be downloaded at: <https://www.mdpi.com/article/10.3390/chemistry4010018/s1>, Figure S1: ^1H NMR (400 MHz, CDCl_3) of compound **1a**, Figure S2: ^{13}C NMR (75 MHz, CDCl_3) of compound **1a**, Figure S3: ESI-MS of compound **1a**, Figure S4: ^1H NMR (400 MHz, CDCl_3) of compound **1b**, Figure S5: ^{13}C NMR (101 MHz, CDCl_3) of compound **1b**, Figure S6: ESI-MS of compound **1b**, Figure S7: ^1H NMR (300 MHz, CDCl_3) of compound **2a**, Figure S8: ^{13}C NMR (75 MHz, CDCl_3) of compound **2a**, Figure S9: ESI-MS of compound **2a**, Figure S10: ^1H NMR (300 MHz, acetone- d_6) of compound **3a**, Figure S11: ^{13}C NMR (75 MHz, acetone- d_6) of compound **3a**, Table S1: Calculation of E factor for molecule **1a**, Table S2: calculation of E factor for molecule **2a**, Table S3: Calculation of E factor for reported IDT precursor, Table S4: Calculation of E factor for reported IDT core (4-hexylaryl substituents), Table S5: Calculation of E factor for the IDT dialdehyde core (hexyl substituents), Table S6: E-factor comparison.

Author Contributions: Conceptualization, G.F., A.N., G.B., R.P. and D.P.; methodology, G.F. and A.N.; investigation, G.F.; writing—original draft preparation, G.F.; writing—review and editing, D.P.; supervision, D.P.; funding acquisition, R.P. and D.P. All authors have read and agreed to the published version of the manuscript.

Funding: This research was funded by ENI S.p.A. (OdL Grant Number 4310359783 and PhD fellowship to G.F.) and MIUR (PRIN 2017 BOOSTER Prot. 2017YXX8AZ).

Institutional Review Board Statement: Not applicable.

Informed Consent Statement: Not applicable.

Data Availability Statement: The data presented in this study are available on request from the corresponding author.

Conflicts of Interest: The authors declare no conflict of interest.

Sample Availability: Samples of the compounds are available from the authors.

References

1. Dauzon, E.; Sallenave, X.; Plesse, C.; Goubard, F.; Amassian, A.; Anthopoulos, T.D. Pushing the Limits of Flexibility and Stretchability of Solar Cells: A Review. *Adv. Mater.* **2021**, *33*, 2101469. [[CrossRef](#)]
2. Seri, M.; Mercuri, F.; Ruani, G.; Feng, Y.; Li, M.; Xu, Z.-X.; Muccini, M. Toward Real Setting Applications of Organic and Perovskite Solar Cells: A Comparative Review. *Energy Technol.* **2021**, *9*, 2000901. [[CrossRef](#)]
3. Yao, J.; Qiu, B.; Zhang, Z.-G.; Xue, L.; Wang, R.; Zhang, C.; Chen, S.; Zhou, Q.; Sun, C.; Yang, C.; et al. Cathode engineering with perylene-diimide interlayer enabling over 17% efficiency single-junction organic solar cells. *Nat. Commun.* **2020**, *11*, 2726. [[CrossRef](#)]
4. Yuan, J.; Zhang, Y.; Zhou, L.; Zhang, G.; Yip, H.-L.; Lau, T.-K.; Lu, X.; Zhu, C.; Peng, H.; Johnson, P.A.; et al. Single-Junction Organic Solar Cell with over 15% Efficiency Using Fused-Ring Acceptor with Electron-Deficient Core. *Joule* **2019**, *3*, 1140–1151. [[CrossRef](#)]
5. Elumalai, N.K.; Uddin, A. Open circuit voltage of organic solar cells: An in-depth review. *Energy Environ. Sci.* **2016**, *9*, 391–410. [[CrossRef](#)]
6. Zhang, H.; Li, Y.; Zhang, X.; Zhang, Y.; Zhou, H. Role of interface properties in organic solar cells: From substrate engineering to bulk-heterojunction interfacial morphology. *Mater. Chem. Front.* **2020**, *4*, 2863–2880. [[CrossRef](#)]
7. Xu, X.; Li, D.; Yuan, J.; Zhou, Y.; Zou, Y. Recent advances in stability of organic solar cells. *EnergyChem* **2021**, *3*, 100046. [[CrossRef](#)]
8. Zheng, Z.; Wang, J.; Bi, P.; Ren, J.; Wang, Y.; Yang, Y.; Liu, X.; Zhang, S.; Hou, J. Tandem Organic Solar Cell with 20.2% Efficiency. *Joule* **2022**, *6*, 171–184. [[CrossRef](#)]
9. Zhao, W.; Li, S.; Yao, H.; Zhang, S.; Zhang, Y.; Yang, B.; Hou, J. Molecular Optimization Enables over 13% Efficiency in Organic Solar Cells. *J. Am. Chem. Soc.* **2017**, *139*, 7148–7151. [[CrossRef](#)]

10. Kolhe, N.B.; West, S.M.; Tran, D.K.; Ding, X.; Kuzuhara, D.; Yoshimoto, N.; Koganezawa, T.; Jenekhe, S.A. Designing High Performance Nonfullerene Electron Acceptors with Rylene Imides for Efficient Organic Photovoltaics. *Chem. Mater.* **2020**, *32*, 195–204. [[CrossRef](#)]
11. Qu, J.; Zhao, Q.; Zhou, J.; Lai, H.; Liu, T.; Li, D.; Chen, W.; Xie, Z.; He, F. Multiple Fused Ring-Based Near-Infrared Nonfullerene Acceptors with an Interpenetrated Charge-Transfer Network. *Chem. Mater.* **2019**, *31*, 1664–1671. [[CrossRef](#)]
12. Li, X.; Li, C.; Ye, L.; Weng, K.; Fu, H.; Ryu, H.S.; Wei, D.; Sun, X.; Woo, H.Y.; Sun, Y. Asymmetric A–D– π –A-type nonfullerene small molecule acceptors for efficient organic solar cells. *J. Mater. Chem. A* **2019**, *7*, 19348–19354. [[CrossRef](#)]
13. Zhang, H.; Yao, H.; Hou, J.; Zhu, J.; Zhang, J.; Li, W.; Yu, R.; Gao, B.; Zhang, S.; Hou, J. Over 14% Efficiency in Organic Solar Cells Enabled by Chlorinated Nonfullerene Small-Molecule Acceptors. *Adv. Mater.* **2018**, *30*, 1800613. [[CrossRef](#)]
14. Liu, Y.; Li, M.; Zhou, X.; Jia, Q.-Q.; Feng, S.; Jiang, P.; Xu, X.; Ma, W.; Li, H.-B.; Bo, Z. Nonfullerene Acceptors with Enhanced Solubility and Ordered Packing for High-Efficiency Polymer Solar Cells. *ACS Energy Lett.* **2018**, *3*, 1832–1839. [[CrossRef](#)]
15. Forti, G.; Nitti, A.; Osw, P.; Bianchi, G.; Po, R.; Pasini, D. Recent Advances in Non-Fullerene Acceptors of the IDIC/ITIC Families for Bulk-Heterojunction Organic Solar Cells. *Int. J. Mol. Sci.* **2020**, *21*, 8085. [[CrossRef](#)] [[PubMed](#)]
16. Lin, Y.; He, Q.; Zhao, F.; Huo, L.; Mai, J.; Lu, X.; Su, C.-J.; Li, T.; Wang, J.; Zhu, J.; et al. A Facile Planar Fused-Ring Electron Acceptor for As-Cast Polymer Solar Cells with 8.71% Efficiency. *J. Am. Chem. Soc.* **2016**, *138*, 2973–2976. [[CrossRef](#)] [[PubMed](#)]
17. Lin, Y.; Wang, J.; Zhang, Z.-G.; Bai, H.; Li, Y.; Zhu, D.; Zhan, X. An Electron Acceptor Challenging Fullerenes for Efficient Polymer Solar Cells. *Adv. Mater.* **2015**, *27*, 1170–1174. [[CrossRef](#)] [[PubMed](#)]
18. Klopp, J.M.; Pasini, D.; Frechet, J.M.J.; Willson, C.G.; Byers, J.D. Microlithographic Assessment of a Novel Family of Transparent and Etch Resistant Chemically Amplified 193 nm Resists Based on Cyclopolymers. *Chem. Mater.* **2001**, *13*, 4147–4153. [[CrossRef](#)]
19. Corsini, F.; Nitti, A.; Tatsi, E.; Mattioli, G.; Botta, C.; Pasini, D.; Griffini, G. Large-Area Semi-Transparent Luminescent Solar Concentrators Based on Large Stokes Shift Aggregation-Induced Fluorinated Emitters Obtained Through a Sustainable Synthetic Approach. *Adv. Opt. Mater.* **2021**, *9*, 2100182. [[CrossRef](#)]
20. Chen, H.; Wadsworth, A.; Ma, C.; Nanni, A.; Zhang, W.; Nikolka, M.; Luci, A.M.T.; Perdigão, L.M.A.; Thorley, K.J.; Cendra, C.; et al. The Effect of Ring Expansion in Thienobenzob[*b*]indacenodithiophene Polymers for Organic Field-Effect Transistors. *J. Am. Chem. Soc.* **2019**, *141*, 18806–18813. [[CrossRef](#)] [[PubMed](#)]
21. Xie, L.; Xiao, J.; Wu, L.; Zhang, W.; Ge, Z.; Tan, S. Synthesis and photovoltaic properties of small molecule electron acceptors with twin spiro-type core structure. *Dyes Pigment.* **2019**, *168*, 197–204. [[CrossRef](#)]
22. Nitti, A.; Bianchi, G.; Po, R.; Pasini, D. Scalable Synthesis of Naphthothiophene and Benzodithiophene Scaffolds as π -Conjugated Synthons for Organic Materials. *Synthesis* **2019**, *51*, 677–682. [[CrossRef](#)]
23. Nitti, A.; Bianchi, G.; Po, R.; Pasini, D. Direct Arylation Strategies in the Synthesis of π -Extended Monomers for Organic Polymeric Solar Cells. *Molecules* **2017**, *22*, 21. [[CrossRef](#)]
24. Zhao, F.; Dai, S.; Wu, Y.; Zhang, Q.; Wang, J.; Jiang, L.; Ling, Q.; Wei, Z.; Ma, W.; You, W.; et al. Single-Junction Binary-Blend Nonfullerene Polymer Solar Cells with 12.1% Efficiency. *Adv. Mater.* **2017**, *29*, 1700144. [[CrossRef](#)]
25. Nitti, A.; Forti, G.; Bianchi, G.; Botta, C.; Tinti, F.; Gazzano, M.; Camaioni, N.; Po, R.; Pasini, D. Anthradithiophene-based organic semiconductors through regiodirected double annulations. *J. Mater. Chem. C* **2021**, *9*, 9302–9308. [[CrossRef](#)]
26. Cui, Y.; Yao, H.; Gao, B.; Qin, Y.; Zhang, S.; Yang, B.; He, C.; Xu, B.; Hou, J. Fine-Tuned Photoactive and Interconnection Layers for Achieving over 13% Efficiency in a Fullerene-Free Tandem Organic Solar Cell. *J. Am. Chem. Soc.* **2017**, *139*, 7302–7309. [[CrossRef](#)]
27. Xie, D.; Liu, T.; Gao, W.; Zhong, C.; Huo, L.; Luo, Z.; Wu, K.; Xiong, W.; Liu, F.; Sun, Y.; et al. A Novel Thiophene-Fused Ending Group Enabling an Excellent Small Molecule Acceptor for High-Performance Fullerene-Free Polymer Solar Cells with 11.8% Efficiency. *Sol. RRL* **2017**, *1*, 1700044. [[CrossRef](#)]
28. Wang, J.; Wang, W.; Wang, X.; Wu, Y.; Zhang, Q.; Yan, C.; Ma, W.; You, W.; Zhan, X. Enhancing Performance of Nonfullerene Acceptors via Side-Chain Conjugation Strategy. *Adv. Mater.* **2017**, *29*, 1702125. [[CrossRef](#)] [[PubMed](#)]
29. Wang, J.; Zhan, X. Fused-Ring Electron Acceptors for Photovoltaics and Beyond. *Acc. Chem. Res.* **2021**, *54*, 132–143. [[CrossRef](#)]
30. Nitti, A.; Bianchi, G.; Po, R.; Porta, A.; Galbiati, A.; Pasini, D. Weiss-Cook Condensations for the Synthesis of Bridged Bithiophene Monomers and Polymers. *ChemistrySelect* **2019**, *4*, 12569–12572. [[CrossRef](#)]
31. Pasini, D.; Klopp, J.M.; Frechet, J.M.J. Design, Synthesis, and Characterization of Carbon-Rich Cyclopolymers for 193nm Microlithography. *Chem. Mater.* **2001**, *13*, 4136–4146. [[CrossRef](#)]
32. Nitti, A.; Osw, P.; Calcagno, G.; Botta, C.; Etkind, S.I.; Bianchi, G.; Po, R.; Swager, T.M.; Pasini, D. One-Pot Regiodirected Annulations for the Rapid Synthesis of π -Extended Oligomers. *Org. Lett.* **2020**, *22*, 3263–3267. [[CrossRef](#)] [[PubMed](#)]
33. Penconi, M.; Bianchi, G.; Nitti, A.; Savoini, A.; Carbonera, C.; Pasini, D.; Po, R.; Luzzati, S. A Donor Polymer with a Good Compromise between Efficiency and Sustainability for Organic Solar Cells. *Adv. Energy Sustain. Res.* **2021**, *2*, 2100069. [[CrossRef](#)]
34. Osw, P.; Nitti, A.; Abdullah, M.N.; Etkind, S.I.; Mwaura, J.; Galbiati, A.; Pasini, D. Synthesis and Evaluation of Scalable D-A-D π -Extended Oligomers as p-Type Organic Materials for Bulk-Heterojunction Solar Cells. *Polymers* **2020**, *12*, 720. [[CrossRef](#)] [[PubMed](#)]
35. Nitti, A.; Osw, P.; Abdullah, M.N.; Galbiati, A.; Pasini, D. Scalable Synthesis of Naphthothiophene-based D- π -D Extended Oligomers through Cascade Direct Arylation Processes. *Synlett* **2018**, *29*, 2577–2581.
36. Nitti, A.; Bianchi, G.; Po, R.; Swager, T.M.; Pasini, D. Domino Direct Arylation and Cross-Aldol for Rapid Construction of Extended Polycyclic π -Scaffolds. *J. Am. Chem. Soc.* **2017**, *139*, 8788–8791. [[CrossRef](#)] [[PubMed](#)]

37. Li, Y.; Tatum, W.K.; Onorato, J.W.; Barajas, S.D.; Yang, Y.Y.; Luscombe, C.K. An indacenodithiophene-based semiconducting polymer with high ductility for stretchable organic electronics. *Polym. Chem.* **2017**, *8*, 5185–5193. [[CrossRef](#)]
38. Wang, C.; Du, T.; Liang, Z.; Zhu, J.; Ren, J.; Deng, Y. Synthesis of low-bandgap small molecules by extending the π -conjugation of the termini in quinoidal compounds. *J. Mater. Chem. C* **2021**, *9*, 2054–2062. [[CrossRef](#)]
39. Zhang, Y.; Zou, J.; Yip, H.-L.; Chen, K.-S.; Zeigler, D.F.; Sun, Y.; Jen, A.K.-Y. Indacenodithiophene and Quinoxaline-Based Conjugated Polymers for Highly Efficient Polymer Solar Cells. *Chem. Mater.* **2011**, *23*, 2289–2291. [[CrossRef](#)]
40. Li, Y.; Liu, X.; Wu, F.-P.; Zhou, Y.; Jiang, Z.-Q.; Song, B.; Xia, Y.; Zhang, Z.-G.; Gao, F.; Inganäs, O.; et al. Non-fullerene acceptor with low energy loss and high external quantum efficiency: Towards high performance polymer solar cells. *J. Mater. Chem. A* **2016**, *4*, 5890–5897. [[CrossRef](#)]
41. Terenti, N.; Petronela Crisan, A.; Jungsuttiwong, S.; Hadade, N.D.; Pop, A.; Grosu, I.; Roncali, J. Effect of the mode of fixation of the thienyl rings on the electronic properties of electron acceptors based on indacenodithiophene (IDT). *Dyes Pigment.* **2021**, *187*, 109116. [[CrossRef](#)]
42. Li, J.-N.; Cui, M.; Dong, J.; Jing, W.; Bao, J.; Liu, Z.; Ma, Z.; Gao, X. Voltage loss analysis of novel non-fullerene acceptors with chlorinated non-conjugated thienyl chains. *Dyes Pigment.* **2021**, *188*, 109162. [[CrossRef](#)]
43. Ming, S.; Liu, Y.; Feng, S.; Jiang, P.; Zhang, C.; Li, M.; Song, J.; Bo, Z. Fused-ring acceptor with a spiro-bridged ladder-type core for organic solar cells. *Dyes Pigment.* **2019**, *163*, 153–158. [[CrossRef](#)]
44. Sheldon, R.A. The E Factor: Fifteen years on. *Green Chem.* **2007**, *9*, 1273–1283. [[CrossRef](#)]
45. Sanzone, A.; Calascibetta, A.; Ghiglietti, E.; Ceriani, C.; Mattioli, G.; Mattiello, S.; Sassi, M.; Beverina, L. Suzuki-Miyaura Micellar One-Pot Synthesis of Symmetrical and Unsymmetrical 4,7-Diaryl-5,6-difluoro-2,1,3-benzothiadiazole Luminescent Derivatives in Water and under Air. *J. Org. Chem.* **2018**, *83*, 15029–15042. [[CrossRef](#)] [[PubMed](#)]